Comparative Landscape of Small RNAs in Tissue and Liquid Biopsies for Liver Transplant Outcomes

Monima Anam[1], Christine Watkins[2], Grace Rucker[2], Katie Marlow[1], Matthew Khalil[2], Murat Dogan[2], James Eason [2,3,4], Jason Vanatta [2,3], Corey Eymard [2,3], Cem Kuscu[2], Zhangli Su*[1], Canan Kuscu*[2]

[1] Department of Genetics, University of Alabama at Birmingham, Birmingham, AL, 35233, United States

[2] Transplant Research Institute, Department of Surgery, University of Tennessee Health Science Center, Memphis, TN, 38163, United States

[3] Methodist University Hospital, Memphis, TN, 38163, United States

[4] Current address: HCA Florida Hospitals, Largo, FL, 33770, United States

*Correspondence: Canan Kuscu (ckuscu@uthsc.edu) and Zhangli Su (zsu@uab.edu)

Abstract:

Background:

Ischemia-reperfusion injury (IRI) is an inevitable consequence of liver transplantation, arising during donor organ procurement and reoxygenation. Severe IRI is a leading contributor to early allograft dysfunction (EAD), a post-transplant complication associated with reduced graft survival. Current postoperative biomarkers provide limited time for intervention, highlighting a need to identify preoperative biomarkers of IRI. Meanwhile,

tRNA fragments (tRFs) have emerged as novel biomarkers in various diseases, but remain unexplored in the context of liver transplant.

Results:

We performed small RNA sequencing on donor liver biopsies to investigate IRI-associated transcript changes. In parallel, donor liver perfusates were analyzed as a non-invasive surrogate for tissue profiling. Across samples, microRNAs (miRNAs) and tRFs were the most abundant small RNAs. Perfusate expression strongly correlated with paired biopsies, supporting its value as a non-invasive source. Comparison of post-reperfusion versus pre-implantation biopsies revealed that IRI reprogrammed tRF expression. Stratification by clinical outcome showed that patients who developed EAD exhibited specific tRNA fragments signature in both biopsy and perfusate. Receiver operating characteristic (ROC) analysis demonstrated that a tRF-based model achieved an AUC of 0.7748, outperforming the donor risk index alone (AUC = 0.6804), representing a 9.4% increase in discriminative capacity.

Conclusions:

These results are the first to establish tRFs as IRI-responsive biomolecules abundant in both donor liver tissue and perfusate, a non-invasive biofluid. In particular, various tRF species emerged as promising candidate biomarkers for early detection of EAD. These results lay the foundation to further investigate the diagnostic and prognostic utility of tRF species in clinical liver transplantation.

Keywords (3-10):

tRFs, non-invasive biomarkers, ischemia-reperfusion injury, early allograft dysfunction, liver transplantation

Background

Ischemia-reperfusion injury (IRI) is an inevitable consequence of solid organ transplantation, initiated during donor organ procurement and cold storage, and exacerbated upon reperfusion in the recipient. The sudden reoxygenation of ischemic tissue induces a complex interplay of oxidative stress, metabolic disturbances, sterile inflammation, and cell death pathways that impair graft integrity (1). Severe IRI is a principal contributor to early allograft dysfunction (EAD), a clinical syndrome presenting within the first week post liver transplant, associated with increased morbidity, primary nonfunction, and diminished long-term graft survival (2). Current diagnostic criteria for EAD primarily rely on postoperative serum biochemical markers such as alanine aminotransferase (ALT) and aspartate aminotransferase (AST), which provide limited mechanistic insight and insufficient lead time for intervention (3). This underscores the need for high-resolution molecular biomarkers capable of detecting early transcriptional and post-transcriptional responses to IRI in graft tissue and accessible biofluids, thereby enabling predictive and mechanism-informed monitoring after liver transplantation.

Small RNAs are central regulators of post-transcriptional gene expression, modulating mRNA stability, translation, and chromatin organization across diverse biological contexts. Beyond well-characterized microRNAs and piRNAs, transfer RNA-derived fragments (tRFs) and stress-induced tRNA halves (tiRs) have recently emerged as abundant and functionally versatile small RNA species generated by precise cleavage of precursor or mature tRNAs (4). Their biogenesis is strongly induced by cellular stressors, including oxidative injury, nutrient deprivation, hypoxia, and immune activation (5,6). Functionally, tRFs repress global protein synthesis, promote stress granule

assembly, displace messenger RNAs from RNA-binding proteins such as YBX1, and participate in RNA silencing pathways via Argonaute association (7–10). A recent publication also demonstrated that hypoxia induced tRF promotes cellular homeostasis and protects against kidney injury by enhancing autophagic flux (11). Through these mechanisms, tRFs act as dynamic modulators of cellular adaptation to stress, influencing survival, metabolism, and signaling, positioning them as promising molecular sentinels of stress phenotypes in both experimental and clinical settings (12,13).

Recent advances in transcriptomic profiling have identified small RNA signatures as a promising class of molecular biomarkers for disease diagnosis, prognosis, and therapeutic monitoring. Their inherent stability in biofluids, resistance to RNase degradation, and ability to reflect dynamic physiological states make them well-suited for minimally invasive diagnostics (14,15). In liver transplantation, liver-specific miR-122 detected in recipient serum was shown to be correlated with ALT and AST levels, thus IRI severity and EAD (16). Furthermore, donor organ preservation solution (perfusate) has emerged as an attractive biospecimen for biomarker discovery, capturing molecules released directly from the donor liver during storage and perfusion (17,18). While these investigations provide important proof-of-concepts, they focused on targeted RNA species rather than unbiased transcriptome-wide profiling. Consequently, the broader RNA repertoire within perfusate, including stress-responsive small RNAs such as tRFs and tiRs, remains largely unexplored. Here, we report the first transcriptome-wide small RNA profiling of liver transplant biopsies alongside perfusate, aimed at uncovering mechanistically linked early non-invasive biomarkers of graft function that complement tissue-based assays.

97 **Results**

98 **Small RNAs and tRFs are abundantly expressed in donor liver transplant biopsy**
99 **samples.**

100 To characterize small RNAs present in donor liver tissue and determine whether
101 they change from pre- to post-transplantation, we collected donor liver biopsy samples at
102 two timepoints: pre-implantation (L1) and post-reperfusion (L2), followed by small RNA
103 sequencing analysis (**Fig. 1A**). Principal component analysis (PCA) revealed distinct
104 separation between L1 and L2 small RNA expression profiles, with PC1 and PC2
105 accounting for 19% and 12% of the variance, respectively (**Fig. 1B).** A variety of small
106 RNA species were detected through sequencing; however, miRNAs comprised the
107 largest proportion of mapped reads, followed by tRFs (**Fig. 1C**), where the top fifty most
108 highly expressed RNAs were exclusively miRNAs or tRFs (**Fig. S1A**). Four tRF subtypes
109 dominated the tRF landscape: tiR5, tRF5, tRF3CCA, and tRF1 species (**Fig. 1D and E**).
110 tiR5s are known as 5' tRNA halves, which are typically 30–35 nucleotides (nt) in length,
111 while tRF5s are shorter 5' tRNA fragments that range from 15–29 nt long. tRF3CCAs are
112 3' tRNA fragments that retain 3' CCA tails, a feature of mature tRNAs. While tRF1s are
113 the remnant 3' trailer sequences that are cleaved from precursor tRNAs to form mature
114 tRNAs. These four tRF subtypes represented the majority of mapped tRF reads across
115 samples. Additionally, tRFs derived from Glu- and Gly-carrying parental tRNAs were
116 highly enriched relative to other amino acid isotypes (**Fig. S1B**). Furthermore, multiple
117 tRF species rivaled the expression of the topmost expressed miRNAs, such as Glu CTC
118 tiR5 and Gly GCC tiR5, which were the fourth- and sixth-most highly expressed small

119 RNAs across samples (**Fig. S1A**). Overall, we observe that tRFs are steadily abundant
120 across L1 and L2 samples, serving as promising candidates for further investigation.
121
122 **Comparison of L2 vs. L1 expression profiles reveals IRI-associated tRF changes.**
123 We next examined small RNAs differentially expressed in response to IRI by
124 comparing L2 and L1 samples, as L2 samples were collected post-reperfusion and
125 therefore serve as a proxy for transplant-associated IRI. DESeq2 analysis of L2 vs. L1
126 small RNA profiles revealed 182 differentially expressed small RNAs, including 116 tRFs
127 and 66 miRNAs (**Supplementary Table 1**). Of these, 102 (58 tRFs, 44 miRNAs) were
128 upregulated and 80 (58 tRFs, 22 miRNAs) were downregulated in L2 compared to L1
129 (**Fig. 2A and B**). Strikingly, tRFs of the same subtype displayed uniform directional
130 changes. Among the most abundant tRF classes, differentially expressed tiR5s were
131 consistently enriched in L2, while significant tRF3CCA species were consistently depleted
132 in L2. Similar trends were observed for differentially expressed tRF1 and tRF5 species,
133 with the majority showing upregulation following IRI (**Fig. 2B**). Boxplots of select tiR5 and
134 tRF3CCA species likewise exemplify and highlight this trend (**Fig. 2C-E**). Together, these
135 findings indicate that IRI is associated with subtype-specific changes in tRF expression,
136 suggesting that tRF dysregulation may be a characteristic feature of IRI.
137
138 **IRI-associated tRF changes are stratified by transplant outcome.**
139 Next, we stratified patients by early transplant outcome to assess whether IRI-
140 associated tRF changes were uniquely associated with graft dysfunction. Transplant
141 outcomes were based on day 1 AST (aspartate aminotransferase) values (2), where high

142 AST values (>2000) corresponded to early allograft dysfunction (EAD, n = 18) and
143 moderate/low AST values corresponded to normal function (NF, n = 30) **(Fig. 3A and**
144 **S2A)**. DESeq2 analysis of L2 vs. L1 in each outcome group (EAD or NF) revealed group-
145 dependent regulation of tRFs. In the EAD group, L2 biopsies showed unique upregulation
146 of numerous tiR5 species not observed in NF samples **(Fig. 3B and C)**. In contrast, the
147 NF group exhibited unique upregulation of multiple tRF1 species in L2 vs. L1 comparisons
148 **(Fig. 3B, S2C and D)**. Notably, no tiR5 species were downregulated in L2 in either group
149 **(Fig. S2E)**. Downregulated RNAs in L2 were largely shared between groups and
150 consisted primarily of tRF3CCA species **(Fig. S2E and F)**. Overall, we observe that post-
151 IRI tRF changes are uniquely dysregulated in EAD and NF grafts, suggesting that tRFs
152 may be prognostically linked to graft outcome.
153
154 **Comparison of EAD vs. NF small RNA profiles reveals transplant outcome-**
155 **associated tRF changes, independent of IRI.**
156 To evaluate whether small RNA profiles differed between EAD and NF grafts, we
157 performed differential expression analysis (EAD vs. NF) separately within L1 and L2
158 samples. This approach allowed us to identify small RNAs associated with transplant
159 outcome independent of IRI-induced changes. DESeq2 analysis revealed multiple
160 differentially expressed small RNAs that were shared across EAD vs. NF comparisons.
161 Specifically, miR-452-5p and miR-224-5p were significantly upregulated in EAD samples
162 compared to NF samples, while Pro CGG tiR5 was downregulated (**Fig. 4A–E and Fig.**
163 **S3A–B**). Although IRI (L2 vs. L1) induced significant increases in Pro CGG tiR5
164 expression, levels remained consistently lower in EAD grafts compared to NF at both

165 timepoints. (**Fig. 4E**). Across both biopsy timepoints, ten miRNAs were commonly
166 upregulated in EAD (**Fig. S3A**). In contrast, five small RNAs were consistently
167 downregulated in EAD, with the majority being tRF3CCA species, alongside one tiR5 and
168 one miRNA species (**Fig. S3B**). Together, these findings demonstrate that small RNA
169 profiles differ between EAD and NF groups, regardless of IRI status, suggesting that pre-
170 implantation profiles may be sufficiently informative to aid in predicting EAD.
171

172 **Pre-transplant liver perfusate is enriched with tRFs and small RNA species.**

173 To determine whether liver biopsy-associated tRF changes could be captured non-
174 invasively, we analyzed small RNAs in donor liver preservation solution (now referred to
175 as perfusate). Donor livers were submerged in preservation solution and transported on
176 ice prior to transplantation. Immediately before implantation, perfusate was collected and
177 analyzed based on EAD (n = 49) and NF (n = 112) presence (**Fig. S4A**). RNA was
178 extracted from the perfusate and a robust signal corresponding to small RNA size was
179 detected after library construction (**Fig. 5A and Fig. S4B**). The size distribution from the
180 perfusate appears different from the one derived from tissue, highlighting specific
181 enrichment of small RNAs in the perfusate. (**Fig. S4B**) As a readily accessible biofluid
182 that does not require tissue biopsy, liver perfusate represents a promising non-invasive
183 source for biomarker discovery. Small RNA sequencing revealed a high abundance of
184 small RNAs in perfusate, with tRFs as the most prevalent class, followed by mitochondrial
185 tRFs (MtRFs) (**Fig. 5B**). Comparisons between perfusates from EAD versus NF donors
186 showed no significant differences in the overall distribution of small RNA classes; tRFs
187 were similarly abundant across both groups (**Fig. 5C).** Despite the lack of global

188 differences, the consistently high levels of tRFs and other small RNAs in perfusate
189 highlight its potential as a platform for identifying novel RNA biomarkers predictive of
190 donor liver quality and transplant outcomes.
191
192 **Pre-transplant perfusate small RNAs are differentially expressed in EAD and may**
193 **help predict transplant outcome.**
194 We next investigated whether pre-transplant perfusate small RNAs reflect donor
195 liver quality and could serve as biomarkers for EAD. Due to the lower complexity of cDNA
196 libraries from perfusate samples, DESeq2 normalization was not suitable; therefore, we
197 quantified expression using reads per million (RPM) and identified differentially expressed
198 small RNAs using Student's T-tests. This analysis revealed multiple small RNAs
199 significantly dysregulated between EAD and NF samples (**Fig. 6A**). Perfusate samples
200 contained a higher proportion of tRFs compared to biopsy tissue, with the most abundant
201 species being tiR5 and tRF5 fragments (**Fig. 6B**). To assess the extent to which perfusate
202 reflects donor liver tissue small RNA profiles, we performed correlation analyses across
203 matched samples. Pearson correlations revealed moderate to strong relationships
204 between perfusate and both L1 (mean R = 0.70) and L2 (mean R = 0.72) biopsy profiles
205 (**Fig. S5A and S5B**), indicating that perfusate partially recapitulates the tissue molecular
206 landscape. We next compared differentially expressed RNAs across perfusate (EAD vs.
207 NF), L2 biopsies (EAD vs. NF), and L1 biopsies (EAD vs. NF) comparisons. Several
208 downregulated RNAs overlapped between perfusate and tissue datasets (**Fig. 6C and**
209 **Fig. S5C**). In particular, three highly expressed Proline-tiR5 species (Pro CGG tiR5, Pro
210 TGG tiR5, and Pro AGG tiR5) were consistently downregulated in EAD perfusates and

211 EAD biopsy tissues. Additionally, Ser TGA tRF1 was downregulated in both perfusate
212 and L2 biopsies (**Fig. 6A and 6C–E**). Given their consistent association with transplant
213 outcome and high expression in perfusate, we constructed a predictive model
214 incorporating these three Proline tiR5s together with Ser TGA tRF1. Receiver operating
215 characteristic (ROC) analysis demonstrated that the tRF-based model achieved an AUC
216 of 0.7582, outperforming the donor risk index alone (AUC = 0.6804). The donor risk index
217 is a quantitative metric developed to assess the risk of graft failure based on specific
218 donor characteristics including donor age, cold ischemia time, cause of death, and race
219 (19). A combined model integrating both perfusate tRFs and the donor risk index further
220 improved predictive capacity (AUC = 0.7748), representing a 9.4% increase over the
221 donor risk index alone (**Fig. 6F**). Finally, we assessed clinical correlations of the identified
222 perfusate tRFs. All four species showed a significant negative correlation with day 1 AST
223 and ALT values, further supporting their association with early graft injury (**Fig. S5D**).
224 Collectively, these findings demonstrate that pre-transplant liver perfusate is a non-
225 invasive source of small RNAs, particularly tRFs, that partially reflect donor liver tissue
226 profiles and are associated with transplant outcome. Perfusate-derived tRFs may thus
227 represent promising non-invasive biomarkers for predicting EAD in liver transplant.
228

229 **Discussion**

230 In this study, we performed small RNA sequencing on donor liver biopsies from 48
231 cases and reported abundant tRFs (**Fig. 1**). Analysis of paired post-reperfusion versus
232 pre-implantation biopsies revealed that ischemia-reperfusion injury increased tiR5 and

233 tRF1 species, alongside a decrease in tRF3CCA (**Fig. 2**). Notably, tiR5 was particularly
234 enriched in post-reperfusion L2 tissues from patients who developed EAD, whereas tRF1
235 upregulation was specific to those with NF graft outcomes (**Fig. 3**). In parallel, comparison
236 of EAD vs NF in L1 and L2 independently highlighted miRNAs and tRFs which are
237 important for EAD pathology (**Fig. 4**). As a proof of concept to use tissue preservation
238 solution perfusate for non-invasive biomarker discovery, we sequenced perfusate small
239 RNAs and observed abundant tRFs that are likely derived from liver tissues (**Fig. 5**).
240 Perfusate sampling further highlighted the abundance of tRFs, with Pro CGG tiR5, Pro
241 TGG tiR5, Pro AGG tiR5, and Ser TGA tRF1 repeatedly downregulated in EAD in both
242 tissues and perfusate (**Fig. 6**). Our integrated analysis of liver biopsies and perfusate
243 revealed that both compartments contain a shared repertoire of small RNAs specifically
244 tRFs, highlighting the utility of these small RNAs as non-invasive biomarkers for IRI and
245 post-transplant outcomes.

246 The observed increase of multiple tiR5 species in L2 (**Fig. 2B-D**) is likely due to
247 the hypoxia and oxidative stress incurred during static cold storage and reperfusion,
248 consistent with the well-established role of tiR5s as stress-induced RNAs, including in
249 hypoxic contexts (4,13). During cellular stress, these tiR5s have been shown to bind to
250 translation initiation factors such as eIF4G/A and displace the eIF4F complex from
251 mRNAs, resulting in global suppression of protein synthesis while permitting selective
252 translation of stress-adaptive transcripts (20). In addition, tiR5s facilitate the assembly of
253 stress granules, sequestering non-essential mRNAs to further conserve resources and
254 prioritize production of proteins critical for survival and recovery (8). Beyond stress
255 adaptation, infection-induced tiR5s have also been implicated in immune activation,

256 particularly through Toll-like receptor 7 interaction (21–23). Given that IRI is characterized
257 as a sterile inflammatory process in which innate immunity plays a central role, the
258 observed tiR5 induction may represent a mechanistic link between cellular stress and
259 immune activation. In particular, the greater tiR5 increase in patients who developed EAD
260 (**Fig. 3B-C**) could indicate more tissue damage or immune activation in those transplants.
261 Conversely, the specific increase in tRF1s upon reperfusion in patients with NF (**Fig. 3B**
262 **and Fig. S2D**) raises the possibility of a protective role for tRF1 that warrants further
263 mechanistic exploration.

264 The identification of tRFs as dominant small RNAs in perfusate is particularly
265 exciting and demonstrates their potential for use in liquid biopsy monitoring (**Fig. 5**). This
266 is particularly important for evaluating marginal organs and machine perfusion settings,
267 where clinically validated, predictive molecular markers are still lacking. Previously,
268 Verhoeven et al. identified mRNAs and microRNAs in graft preservation solution
269 (perfusate) correlating with early injury (17), while Matton et al. reported that miRNA
270 profiles in normothermic perfusion solution could inform liver viability assessments (18).
271 Both studies were limited to targeted approaches. Our application of unbiased, next-
272 generation sequencing to perfusate along with tissue small RNA profiling identified four
273 clinically relevant tRFs (**Fig. 6C**). Proline-derived tiR5s display diverse, context-
274 dependent functions, ranging from enhancing translation and myeloid differentiation in
275 the bone marrow niche (Pro CGG tiR5) (24) to driving oncogenesis through HPSE2
276 suppression in serrated pathway colorectal cancer (Pro TGG tiR5) (25), while a
277 constitutively expressed Pro tiR5 directly associates with ribosomes to inhibit protein
278 synthesis (26). Ser TGA tRF1 (also known as tRF-1001) suppresses proliferation by

279 inducing G2 arrest in colorectal cancer cells (27), but promotes proliferation and stemness
280 in breast cancer (28), with its levels responsive to nutrient stress. This loss of potential
281 protective tRF signaling in liver tissues may compromise hepatocellular stress adaptation
282 during ischemia–reperfusion, predisposing grafts to dysfunction. Moreover, the
283 expression levels of these four tRFs predicted EAD occurrence better than donor risk
284 index scores, highlighting their clinical potential. In summary, this unbiased study expands
285 the known repertoire of extracellular small RNAs and positions tRFs as strong candidates
286 for rapid, minimally invasive assessment of graft quality during ex situ organ preservation.
287

288 **Conclusion**

289 This study provides the first transcriptome-wide characterization of tRFs in both
290 human liver tissue and donor organ perfusate during transplantation. We demonstrate
291 that specific tRFs, particularly tiR5, are closely linked to reperfusion and EAD, whereas
292 tRF1 appears to be associated with favorable graft outcomes. The prevalence of tRFs in
293 perfusate highlights their potential as non-invasive biomarkers, bridging molecular
294 insights from tissue with clinically accessible diagnostics. By uncovering both shared and
295 compartment-specific signatures, our findings lay a foundation for future validation in
296 larger cohorts and under machine perfusion, advancing tRFs toward clinical application
297 for improved organ assessment and transplant precision.

298

299

Figures and Figure legends

Figure 1

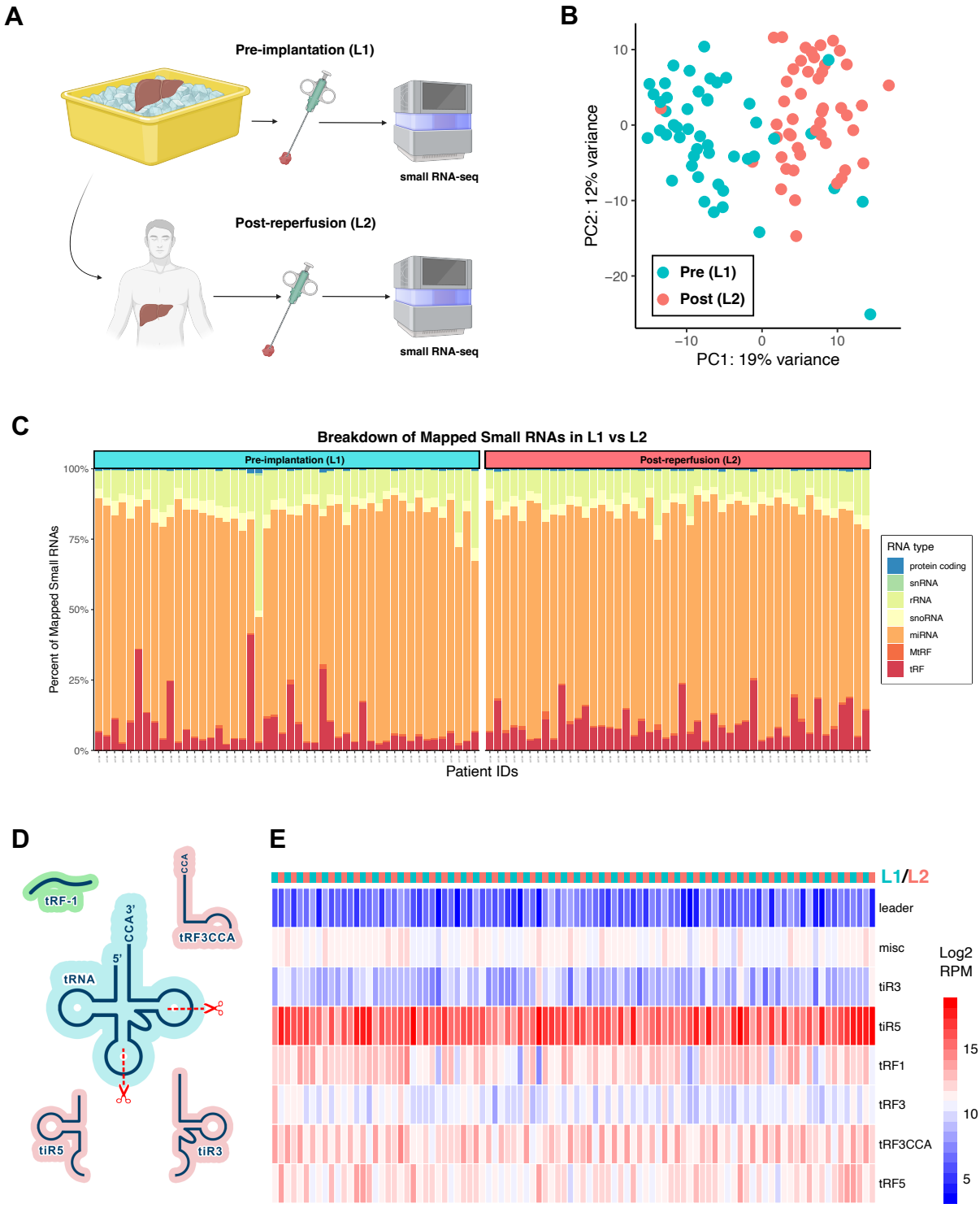

302 **Figure 1. Abundance of tRNA fragments (tRFs) in donor liver transplant biopsy**
303 **samples.**
304 **(A)** Liver biopsy samples were obtained from donor livers at two time points: pre-
305 implantation (L1) and post-reperfusion (L2), followed by small RNA sequencing. **(B)**
306 Principal component analysis (PCA) of small RNA sequencing data reveals distinct
307 clustering between L1 and L2 small RNA profiles. **(C)** Stacked bar plot displaying the
308 proportion of mapped reads for each small RNA type in L1 and L2 samples. For each
309 patient (x-axis), the bars represent the relative proportion of total reads (y-axis) assigned
310 to each small RNA type. Across samples, miRNAs comprised the largest majority of
311 mapped reads, followed by tRFs. **(D)** Schematic illustrating four highlighted tRF subtypes.
312 The tRF nomenclature echoes the region of tRNA from which tRFs are derived. The
313 fragments shown are examples of each tRF subtype and do not represent all possible
314 variants. tRF-1 species (green) are derived from precursor tRNAs (not pictured), while
315 tiR5, tiR3, and tRF3CCA species (pink) are cleaved from mature tRNAs (blue). **(E)**
316 Heatmap displaying the relative expression (Log2 RPM) of different tRF subtypes across
317 L1 and L2 samples. Overall, biopsy samples showed abundant tRF expression.

Figure 2

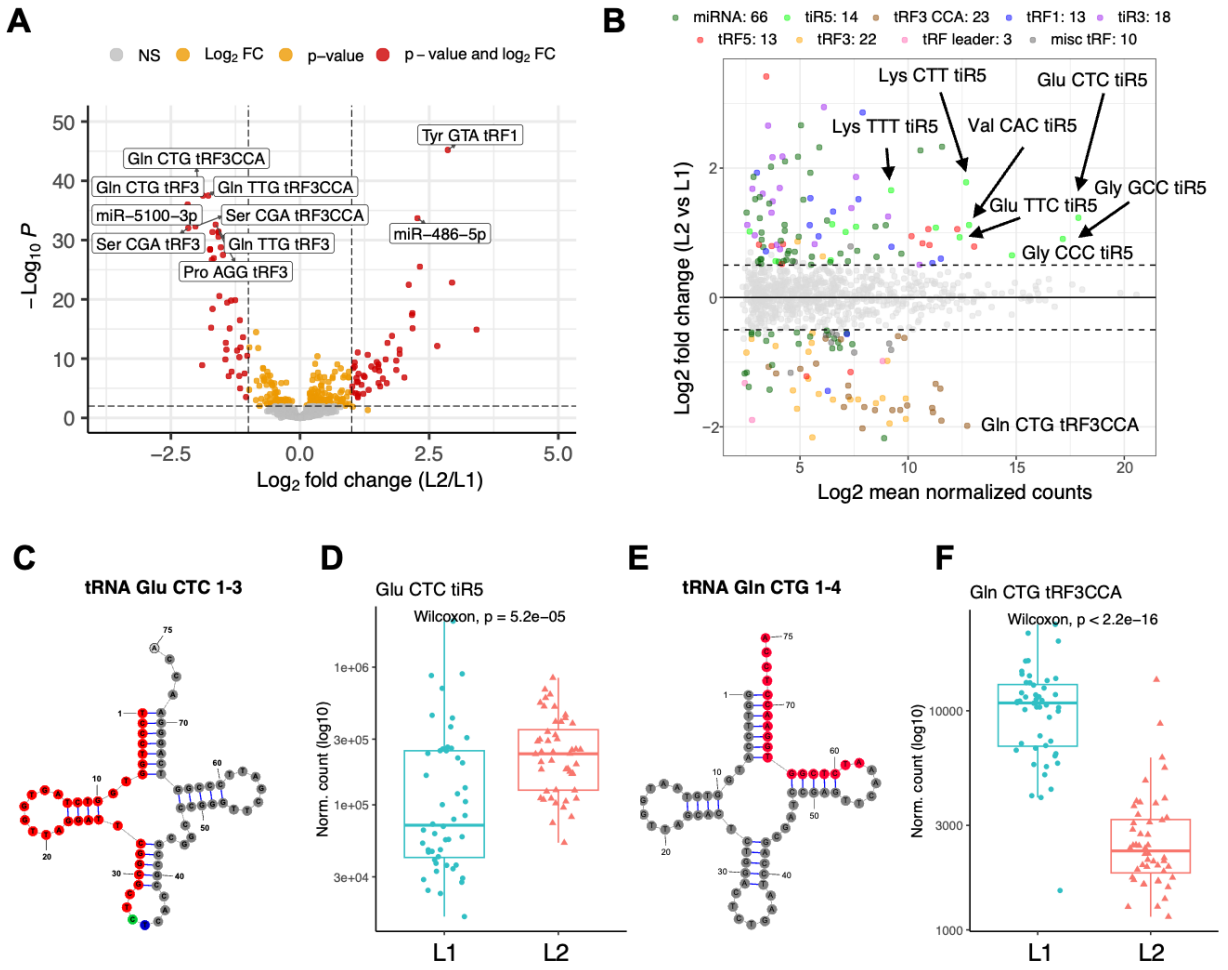

Figure 2. Significant tRF alterations associated with ischemia-reperfusion injury (IRI) during liver transplantation.

(A) Volcano plot of differentially expressed small RNAs between L2 and L1 samples, identified using DESeq2. The x-axis shows the log2 fold change (L2 vs. L1), and the y-axis shows statistical significance (-log10 adjusted p-value). The top 10 most significantly altered small RNAs are labeled, many being tRF3CCA species downregulated in L2. **(B)** MA plot of differentially expressed small RNAs (L2 vs. L1) identified using DESeq2. The x-axis represents gene expression (log2 normalized counts), and the y-axis shows the

327 log2 fold change. Differentially expressed RNAs are color-coded by RNA type (tRF
328 subtype or miRNA). Select highly abundant, significantly altered tRFs are labeled,
329 including many tiR5 species that are upregulated in L2. **(C)** Primary and secondary
330 structure of parental tRNA-Glu-CTC-1-3, with its most abundant tiR5 fragment highlighted
331 in red (positions 1-35). Cleavage sites that generate the second and third most abundant
332 Glu CTC tiR5 isoforms from tRNA-Glu-CTC are marked in green and blue. **D)** Boxplot of
333 Glu CTC tiR5 expression in L1 vs. L2 samples, showing significant upregulation in L2,
334 consistent with IRI-associated induction. **(E)** Primary and secondary structure of parental
335 tRNA-Gln-CTG-1-4, with its corresponding tRF3CCA fragment highlighted in red
336 (positions 58–75). **(F)** Boxplot of Gln CTG tRF3CCA expression in L1 vs. L2 samples,
337 showing significant downregulation in L2, indicative of IRI-associated suppression.

Figure 3

A

L1/L2 Biopsy sample summary (n = 48)

Group	EAD	NF	p value
Number of patients	18	30	
Recipient mean age	57.3	56.6	N.S.
Recipient gender (F/M)	7/11	10/19	N.S.
Donor mean age	47.4	37.7	0.012 *
Donor gender (F/M)	9/9	16/14	N.S.
Mean CIT (hours)	4.89	4.34	N.S.
Mean AST (Day 1)	5472.8	1072.4	2.7e-04 ***
Mean ALT (Day 1)	1618.3	542.5	0.0015 **

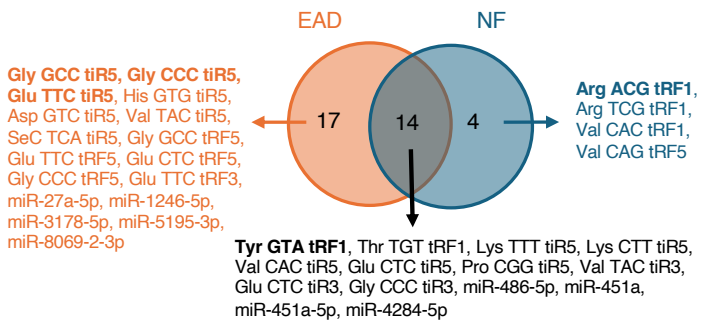

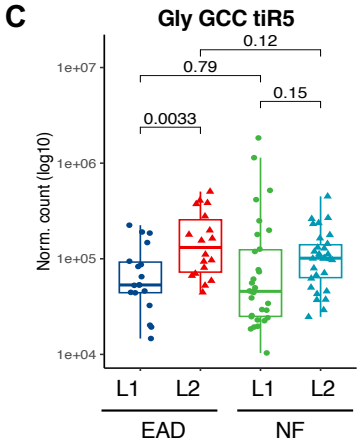

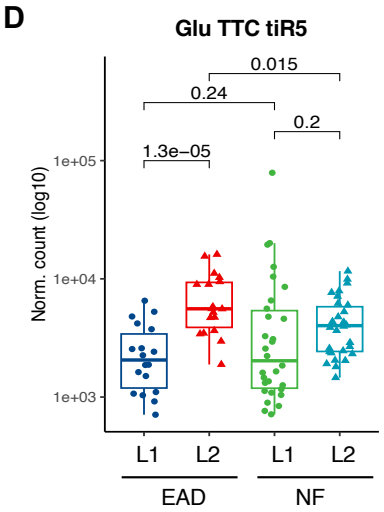

338

339 **Figure 3. IRI-associated tRF alterations are transplant outcome specific.**

340 **(A)** Clinical and demographic characteristics of the patient cohort, stratified by transplant

341 outcome (EAD or NF), which was classified based on day 1 post-transplant aspartate

342 aminotransferase (AST) levels. Cold ischemia time (CIT), the duration the donor liver

343 remained on ice prior to transplantation, averaged 4.6 hours across groups. **(B)**

344 Differential expression analysis of L2 vs. L1 samples was performed separately within

345 EAD and NF groups. The Venn diagram displays small RNAs upregulated in L2 relative

346 to L1 for each group. In the EAD group, uniquely upregulated RNAs were predominantly
347 tiR5 species, whereas in the NF group, uniquely upregulated RNAs were mainly tRF1
348 species. A subset of tiR5 and tRF1 species was commonly upregulated in both groups,
349 alongside other tRF and miRNA species. **(C)** and **(D)** Boxplots showing normalized
350 expression (log10 transformed) of representative tiR5 species (Gly-GCC and Glu-TTC),
351 stratified by transplant outcome (EAD vs. NF) and biopsy timepoint (L2 vs. L1). Statistical
352 comparisons were performed using Wilcoxon rank-sum tests; p-values are indicated
353 above comparisons. Both panels exemplify the EAD-specific upregulation of tiR5s,
354 showing significant upregulation in L2 compared to L1 exclusively in EAD samples
355 (Student's t-test).
356

Figure 4

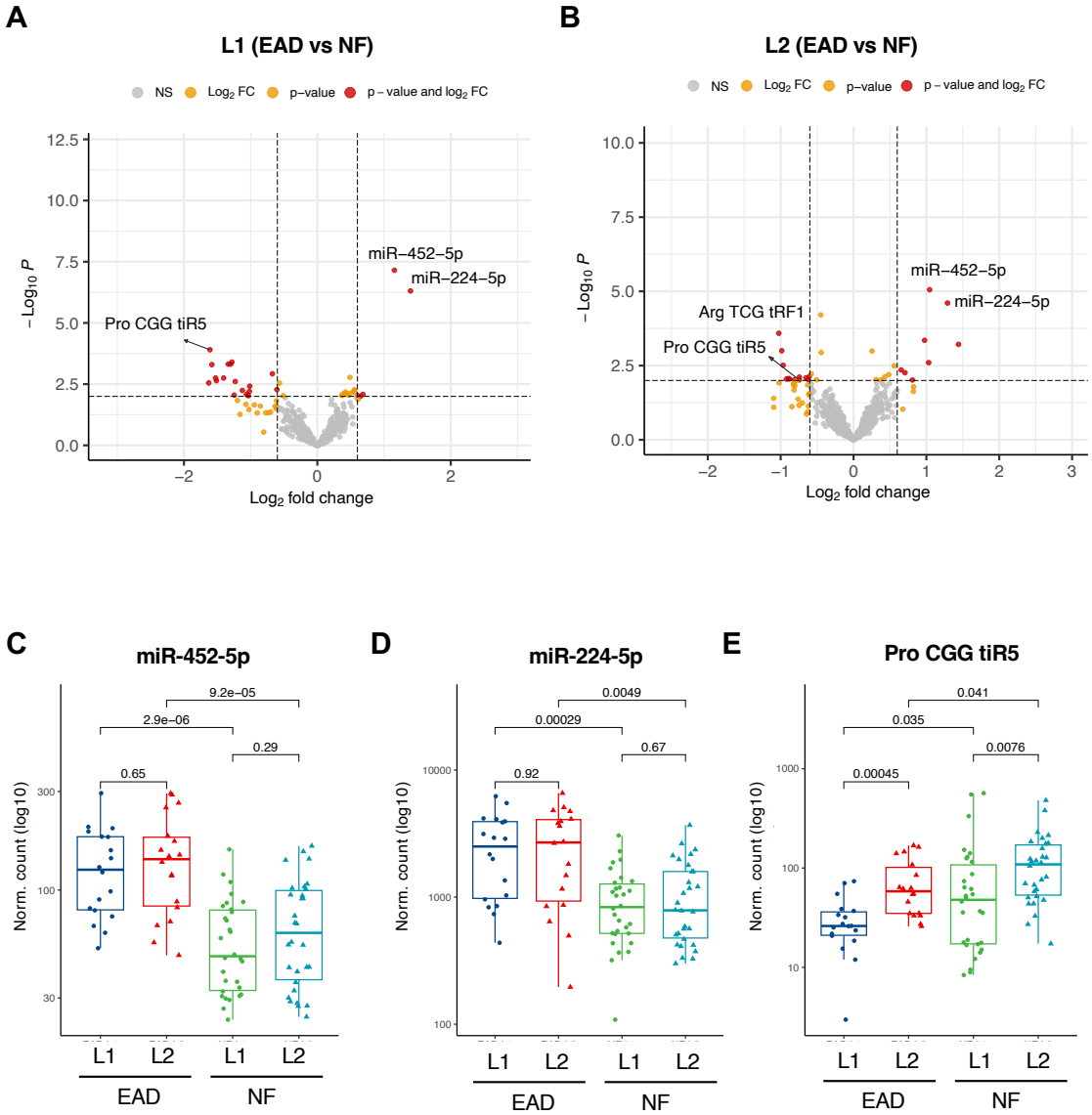

Figure 4. Transplant outcome-associated differences in liver biopsy small RNA expression.

(A) Volcano plot of differentially expressed small RNAs between early EAD and NF in L1 samples, identified using DESeq2. The x-axis represents log2 fold change (EAD vs. NF), and the y-axis indicates statistical significance (−log10 adjusted p-value). The top three most significantly altered small RNAs are labeled. **(B)** Volcano plot of differentially

364 expressed small RNAs between EAD and NF in L2 biopsy samples. The top four most
365 significantly altered small RNAs are labeled. **(C)** and **(D)** Boxplots of normalized
366 expression (log10 transformed) of representative miRNAs (miR-452-5p and miR-224-5p),
367 stratified by transplant outcome (EAD vs. NF) and biopsy timepoint (L1 vs. L2). Both
368 miRNAs are consistently upregulated in EAD compared to NF, independent of time point.
369 Statistical comparisons were performed using Wilcoxon rank-sum tests; p-values are
370 shown above comparisons. **(E)** Boxplots of Pro CGG tiR5 expression, stratified by
371 transplant outcome and biopsy timepoint. While Pro GCC tiR5 expression increases after
372 reperfusion injury (L2 vs. L1), expression remains significantly lower in EAD samples
373 compared to NF at both timepoints (Student's t-test).
374

Figure 5

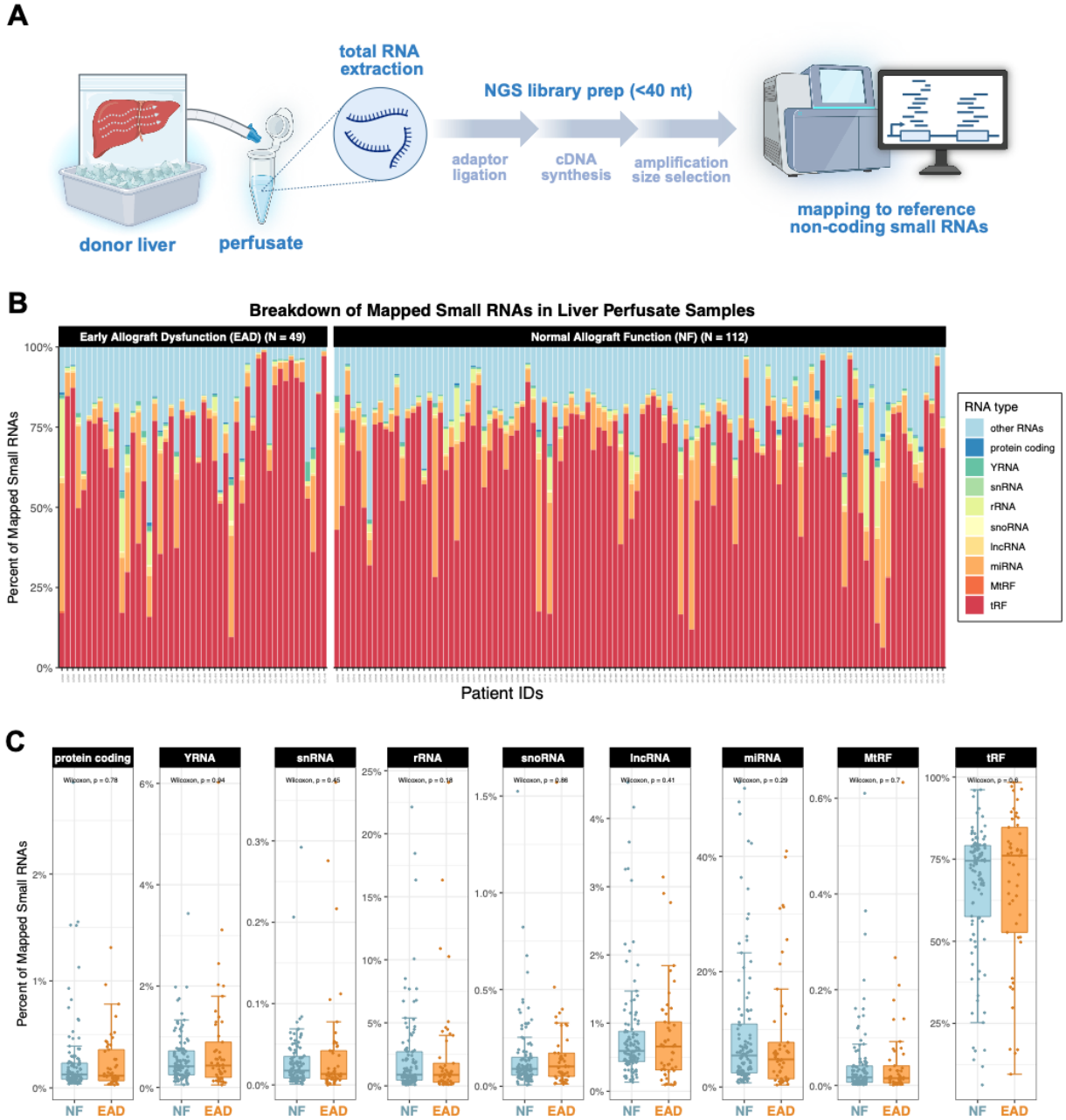

Figure 5. Pre-transplant liver perfusate solution is enriched with small RNAs. **(A)** Donor livers were transported on ice in organ preservation solution prior to transplantation. Immediately before transplantation, the preservation solution (perfusate) was collected, and RNA was isolated for small RNA sequencing**. (B)** Composition of

380 mapped small RNAs in liver perfusate samples, stratified by EAD and NF groups. Across
381 both groups, tRFs represented the predominant RNA species, followed by mitochondrial
382 tRFs (MtRFs). **(C)** Relative abundance of mapped small RNA classes in liver perfusate
383 samples, stratified by NF and EAD groups. Each boxplot displays the percentage of total
384 mapped small RNAs in each class, with each point representing an individual sample.
385 RNA classes were similarly abundant in both EAD and NF samples, with no statistically
386 significant difference between groups (Wilcoxon test).
387

Figure 6

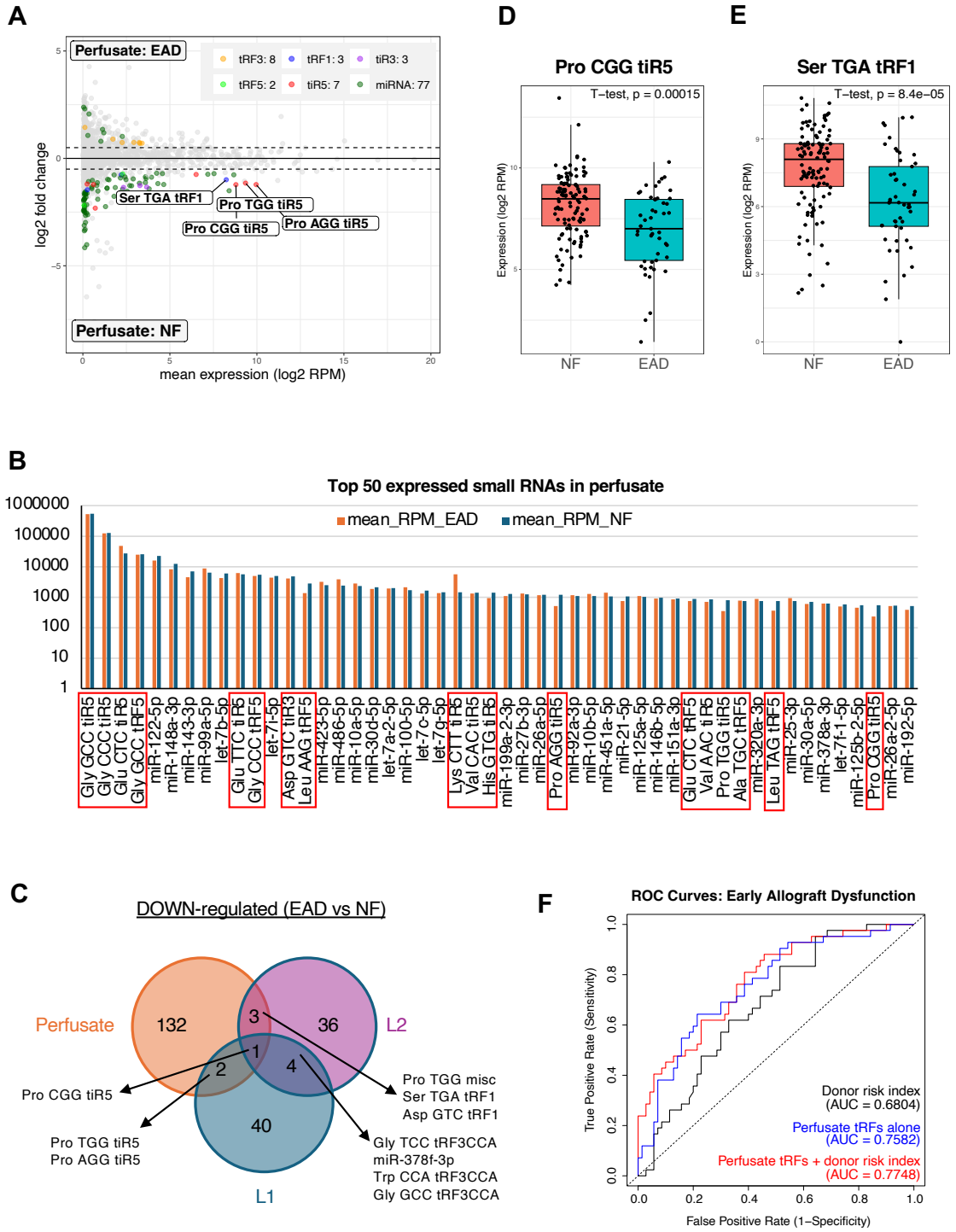

Figure 6. Pre-transplant perfusate small RNAs are differentially expressed based on transplant outcome.

(**A)** MA plot depicting differentially expressed small RNAs (EAD vs. NF) from pre-transplant liver perfusate samples identified using Student's T-test. The x-axis represents gene expression (log2 RPM), and the y-axis shows the log2 fold change. Significantly differentially expressed RNAs are color-coded by RNA type (tRF subtype or miRNA). Select highly abundant, significantly altered tRFs are labeled, including multiple proline-tiR5 species that are downregulated in EAD**. (B)** Bar plot displaying the expression (mean RPM) of the top fifty most highly expressed small RNAs in donor liver perfusate samples, stratified by transplant outcome (EAD (orange) or NF (blue)). These top fifty genes consist entirely of miRNAs and tRFs, which are outlined in red**. (C)** Venn diagram comparing downregulated small RNAs in three comparisons: perfusate EAD vs. NF, L2 EAD vs. NF, and L1 EAD vs. NF. One species, Pro CGG tiR5, was consistently downregulated across all three comparisons, suggesting potential relevance in EAD. Additionally, two other proline-tiR5 species (Pro TGG and Pro AGG) were commonly downregulated in EAD in perfusate and L1 biopsy samples. **(D)** and **(E)** Boxplots showing normalized expression (log2 RPM) of representative tRF species (Pro-CGG-tiR5 and Ser-TGA-tRF1) stratified by transplant outcome (EAD vs. NF) in liver perfusate samples, where these tRFs were significantly downregulated in grafts that developed EAD. Statistical comparisons were performed using Student's T-tests; p-values are indicated above comparisons. **(F)** ROC analysis evaluating the transplant-outcome predictive capacity of three models: donor risk index (black), perfusate tRFs (blue), and a combined model incorporating both perfusate tRFs and donor risk index (red). The donor risk index includes donor age, cold ischemia time, cause of death, and race. The tRF model incorporates the expression of three Pro tiR5s and Ser TGA tRF1 in pre-transplant perfusate. The resulting AUCs were 0.6804

414 (donor risk index), 0.7582 (tRFs), and 0.7748 (combined model), indicating that the
415 addition of perfusate tRFs improved the model's discriminatory capacity for EAD.

416 **Methods**

417 Patient recruitment and specimen collection

418 Liver tissue and perfusate samples were obtained from adult orthotopic liver transplant
419 (OLT) recipients (≥18 years old) at Methodist University Hospital after obtaining informed
420 consent. All procedures were conducted under protocols approved by the University of
421 Tennessee Health Science Center Institutional Review Board (IRB#20-07742-XM and
422 IRB#20-07640-XP).

423 Needle biopsy specimens were immediately immersed in RNA*later* (Thermo Fisher
424 Scientific, Cat. #AM7021) and incubated at 4 °C overnight to ensure complete permeation.
425 RNA*later* was then removed, and the samples were stored at –80 °C until RNA extraction.
426 Perfusate samples were collected at the end of organ procurement concurrently with pre-
427 implantation liver (L1) biopsies. The solutions were centrifuged at 2,400 rpm for 30
428 minutes at room temperature to remove debris. The resulting supernatant was aliquoted
429 and stored at –80 °C until RNA isolation.

430

431 RNA isolation and small RNA library preparation

432 Total RNA was extracted from needle biopsies using the Direct-zol RNA MicroPrep Kit
433 (Zymo Research, Cat. #R2062) according to the manufacturer's instructions, including
434 on-column DNase I treatment to remove genomic DNA contamination. For DOPS
435 samples, RNA was isolated from 500 µl of solution using the same kit, following the
436 manufacturer's protocol for liquid samples, and eluted in 15 µl of RNase-free water.
437 Purified RNA was stored at –80 °C, and repeated freeze–thaw cycles were avoided to
438 minimize RNA degradation.

439 Small RNA libraries were prepared using the NEBNext Multiplex Small RNA Library Prep
440 Set for Illumina (New England Biolabs, Cat. #E7330) following the manufacturer's
441 instructions. For each sample, 100 ng of tissue RNA or 5 µl of DOPS RNA was used as
442 input. Indexing was performed using the NEBNext Multiplex Oligos for Illumina, with PCR
443 amplification carried out for 15 cycles for tissue RNA libraries and 18 cycles for perfusate
444 RNA libraries. Amplified products were resolved on an 8% polyacrylamide gel (Thermo
445 Fisher Scientific, Cat. #EC6215BOX), and target bands were excised and purified. Equal
446 amounts of libraries were pooled and sequenced on an Illumina NextSeq 500 platform,
447 generating approximately 10 million 75 bp single-end reads per sample.
448
449 Small RNA-seq data analysis
450 Raw small RNA sequencing reads were trimmed to remove adapter sequences using
451 Cutadapt (v5.1). Adapter-trimmed reads were then mapped and annotated using Unitas
452 (v1.7.3), a specialized tool for comprehensive small RNA annotation. For liver biopsy
453 samples, read count matrices generated by Unitas were imported into DESeq2 (v1.44.0)
454 in R for normalization and differential expression analysis. Prior to analysis, RNAs with
455 zero counts in more than 80% of samples were excluded to reduce low-abundance noise.
456 Data visualization was performed in R using ggplot2 (v3.5.1) and ggpubr (v0.6.0). For
457 perfusate samples, read count matrices generated by Unitas were imported into R and
458 normalized to reads per million (RPM). Given the lower complexity of perfusate libraries
459 relative to biopsy samples, differential expression analysis was performed using Student's
460 t-tests on RPM values. Data visualization was carried out in R with ggplot2 (v3.5.1) and

ggpubr (v0.6.0), and receiver operating characteristic (ROC) curves were generated using the ROCR package (v1.0-11).

Declarations

Ethics approval and consent to participate

This study was conducted in accordance with the ethical standards of the University of Tennessee Health Science Center Institutional Review Board, which approved all protocols (IRB#20-07742-XM and IRB#20-07640-XP). Liver tissue and perfusate samples were obtained from adult orthotopic liver transplant (OLT) recipients (≥18 years old) at Methodist University Hospital after written informed consent was obtained from all participants.

Availability of data and materials

The small RNA-seq data will be deposited to GEO.

Competing interests

The authors have no competing interests to declare.

Funding

This research was supported by NIH grants R00CA259526 (to Z.S.), T32NS121721 (to M.A.), T32GM135028 (to K.M.), and Transplant Research Institute at UTHSC start up fund (to C.K.).

484 Authors' contributions

485 C.W., G.R., and M.K. helped with patient sample processing, RNA isolation and small
486 RNA library preparation. M.D. and Cem K. coordinated sample collection, storage and
487 contributed to study design. J.E., J.V., and C.E. coordinated patient recruitment and
488 sample collection at the Methodist Hospital. M.A., K.M. and Z.S. performed data analysis
489 on RNA-seq. Canan K. and Z.S. supervised the study and wrote the manuscript with the
490 help of M.A and K.M. All authors read and approved the final manuscript.

491

492 Acknowledgements

493 We would like to thank the Methodist University Hospital transplant team for their
494 assistance with patient recruitment, sample and clinical data collection. We are deeply
495 grateful to the patients and their families for their participation and generous donations to
496 this research. We also would like to acknowledge our colleagues at the Transplant
497 Research Institute for their helpful discussions and ongoing support. We would like to
498 thank IT Research Computing Team at the University of Alabama at Birmingham for NGS
499 support.

500 **References**

501 1. Zhai Y, Petrowsky H, Hong JC, Busuttil RW, Kupiec-Weglinski JW. Ischaemia-
502 reperfusion injury in liver transplantation--from bench to bedside. Nat Rev
503 Gastroenterol Hepatol. 2013 Feb;10(2):79–89.

504 2. Olthoff KM, Kulik L, Samstein B, Kaminski M, Abecassis M, Emond J, et al. Validation
505 of a current definition of early allograft dysfunction in liver transplant recipients and
506 analysis of risk factors. Liver Transpl. 2010 Aug;16(8):943–9.

507 3. Giraudi PJ, Codotto G, Baccarani U, Baralle F, Gondolesi G, Licastro D, et al.
508 Ischemia/Reperfusion Injury and Outcomes in Liver Transplantation Assessed by
509 Omics Technologies: Where Do We Stand? Transplantation. 2025 Aug 13;

510 4. Kumar P, Kuscu C, Dutta A. Biogenesis and Function of Transfer RNA-Related
511 Fragments (tRFs). Trends Biochem Sci. 2016 Aug;41(8):679–89.

512 5. Li G, Manning AC, Bagi A, Yang X, Gokulnath P, Spanos M, et al. Distinct Stress-
513 Dependent Signatures of Cellular and Extracellular tRNA-Derived Small RNAs. Adv
514 Sci (Weinh). 2022 Jun;9(17):e2200829.

515 6. Su Z, Wilson B, Kumar P, Dutta A. Noncanonical Roles of tRNAs: tRNA Fragments
516 and Beyond. Annu Rev Genet. 2020 Nov 23;54:47–69.

517 7. Gebetsberger J, Wyss L, Mleczko AM, Reuther J, Polacek N. A tRNA-derived
518 fragment competes with mRNA for ribosome binding and regulates translation during
519 stress. RNA Biol. 2016 Nov 28;14(10):1364–73.

520 8. Emara MM, Ivanov P, Hickman T, Dawra N, Tisdale S, Kedersha N, et al. Angiogenin-
521 induced tRNA-derived Stress-induced RNAs Promote Stress-induced Stress Granule
522 Assembly. J Biol Chem. 2010 Apr 2;285(14):10959–68.

523 9. Goodarzi H, Liu X, Nguyen HCB, Zhang S, Fish L, Tavazoie SF. Endogenous tRNA-
524 Derived Fragments Suppress Breast Cancer Progression via YBX1 Displacement.
525 Cell. 2015 May 7;161(4):790–802.

526 10. Kuscu C, Kumar P, Kiran M, Su Z, Malik A, Dutta A. tRNA fragments (tRFs) guide Ago
527 to regulate gene expression post-transcriptionally in a Dicer-independent manner.
528 RNA. 2018 Aug;24(8):1093–105.

529 11. Li G, Sun L, Xin C, Hao T, Kharel P, Manning AC, et al. A hypoxia-responsive tRNA-
530 derived small RNA confers renal protection through RNA autophagy. Science. 2025
531 Aug 28;389(6763):eadp5384.

532 12. Anderson P, Ivanov P. tRNA fragments in human health and disease. FEBS Lett.
533 2014 Nov 28;588(23):4297–304.

534 13. Pandey KK, Madhry D, Ravi Kumar YS, Malvankar S, Sapra L, Srivastava RK, et al.
535 Regulatory roles of tRNA-derived RNA fragments in human pathophysiology. Mol
536 Ther Nucleic Acids. 2021 Dec 3;26:161–73.

537 14. Costa B, Li Calzi M, Castellano M, Blanco V, Cuevasanta E, Litvan I, et al. Nicked
538 tRNAs are stable reservoirs of tRNA halves in cells and biofluids. Proc Natl Acad Sci
539 U S A. 2023 Jan 24;120(4):e2216330120.

540 15. Srinivasan S, Yeri A, Cheah PS, Chung A, Danielson K, De Hoff P, et al. Small RNA
541 Sequencing across Diverse Biofluids Identifies Optimal Methods for exRNA Isolation.
542 Cell. 2019 Apr 4;177(2):446-462.e16.

543 16. Farid WRR, Pan Q, van der Meer AJP, de Ruiter PE, Ramakrishnaiah V, de Jonge J,
544 et al. Hepatocyte-derived microRNAs as serum biomarkers of hepatic injury and
545 rejection after liver transplantation. Liver Transpl. 2012 Mar;18(3):290–7.

546 17. Khorsandi SE, Quaglia A, Salehi S, Jassem W, Vilca-Melendez H, Prachalias A, et al.
547 The microRNA Expression Profile in Donation after Cardiac Death (DCD) Livers and
548 Its Ability to Identify Primary Non Function. PLOS ONE. 2015 May 15;10(5):e0127073.

549 18. Matton APM, Selten JW, Roest HP, de Jonge J, IJzermans JNM, de Meijer VE, et al.
550 Cell-free microRNAs as early predictors of graft viability during ex vivo normothermic
551 machine perfusion of human donor livers. Clin Transplant. 2020 Mar;34(3):e13790.

552 19. Feng S, Goodrich NP, Bragg-Gresham JL, Dykstra DM, Punch JD, DebRoy MA, et al.
553 Characteristics associated with liver graft failure: the concept of a donor risk index.
554 Am J Transplant. 2006 Apr;6(4):783–90.

555 20. Ivanov P, Emara MM, Villen J, Gygi SP, Anderson P. Angiogenin-induced tRNA
556 fragments inhibit translation initiation. Mol Cell. 2011 Aug 19;43(4):613–23.

557 21. Pawar K, Kawamura T, Kirino Y. The tRNAVal half: A strong endogenous Toll-like
558 receptor 7 ligand with a 5'-terminal universal sequence signature. Proc Natl Acad Sci
559 U S A. 2024 May 7;121(19):e2319569121.

560 22. Pawar K, Shigematsu M, Sharbati S, Kirino Y. Infection-induced 5′-half molecules of
561 tRNAHisGUG activate Toll-like receptor 7. PLOS Biology. 2020 Dec
562 17;18(12):e3000982.

563 23. Yu J, Zhang X, Cai C, Zhou T, Chen Q. Small RNA and Toll-like receptor interactions:
564 origins and disease mechanisms. Trends Biochem Sci. 2025 May;50(5):385–401.

565 24. Kfoury YS, Ji F, Mazzola M, Sykes DB, Scherer AK, Anselmo A, et al. tiRNA signaling
566 via stress-regulated vesicle transfer in the hematopoietic niche. Cell Stem Cell. 2021
567 Dec 2;28(12):2090-2103.e9.

568 25. Wang XY, Zhou YJ, Chen HY, Chen JN, Chen SS, Chen HM, et al. 5'tiRNA-Pro-TGG,
569 a novel tRNA halve, promotes oncogenesis in sessile serrated lesions and serrated
570 pathway of colorectal cancer. World J Gastrointest Oncol. 2023 Jun 15;15(6):1005–
571 18.

572 26. Gonskikh Y, Gerstl M, Kos M, Borth N, Schosserer M, Grillari J, et al. Modulation of
573 mammalian translation by a ribosome-associated tRNA half. RNA Biol. 2020
574 Aug;17(8):1125–36.

575 27. Lee YS, Shibata Y, Malhotra A, Dutta A. A novel class of small RNAs: tRNA-derived
576 RNA fragments (tRFs). Genes Dev. 2009 Nov 15;23(22):2639–49.

577 28. Wan X, Shi W, Ma L, Wang L, Zheng R, He J, et al. A 3′-pre-tRNA-derived small
578 RNA tRF-1-Ser regulated by 25(OH)D promotes proliferation and stemness by

579 inhibiting the function of MBNL1 in breast cancer. Clin Transl Med. 2024 May
580 9;14(5):e1681.

581